EBioMedicine 16 (2017) 51–62

Contents lists available at ScienceDirect

EBioMedicine

journal homepage: www.ebiomedicine.com

Research Paper

FASN Inhibition and Taxane Treatment Combine to Enhance Anti-tumor Efficacy in Diverse Xenograft Tumor Models through Disruption of Tubulin Palmitoylation and Microtubule Organization and FASN Inhibition-Mediated Effects on Oncogenic Signaling and Gene Expression

Timothy S. Heuer *, Richard Ventura, Kasia Mordec, Julie Lai, Marina Fridlib, Douglas Buckley, George Kemble

3-V Biosciences, Menlo Park, CA, USA

ARTICLE INFO

Article history:
Received 25 August 2016
Received in revised form 19 December 2016
Accepted 20 December 2016
Available online 24 December 2016

Keywords:
Fatty acid synthase
Inhibitor
Paclitaxel
Docetaxel, combination
Palmitoylation

ABSTRACT

Palmitate, the enzymatic product of FASN, and palmitate-derived lipids support cell metabolism, membrane architecture, protein localization, and intracellular signaling. Tubulins are among many proteins that are modified post-translationally by acylation with palmitate. We show that FASN inhibition with TVB-3166 or TVB-3664 significantly reduces tubulin palmitoylation and mRNA expression. Disrupted microtubule organization in tumor cells is an additional consequence of FASN inhibition. FASN inhibition combined with taxane treatment enhances inhibition of in vitro tumor cell growth compared to treatment with either agent alone. In lung, ovarian, prostate, and pancreatic tumor xenograft studies, FASN inhibition and paclitaxel or docetaxel combine to inhibit xenograft tumor growth with significantly enhanced anti-tumor activity. Tumor regression was observed in 3 of 6 tumor xenograft models. FASN inhibition does not affect cellular taxane concentration in vitro. Our data suggest a mechanism of enhanced anti-tumor activity of the FASN and taxane drug combination that includes inhibition of tubulin palmitoylation and disruption of microtubule organization in tumor cells, as well as a sensitization of tumor cells to FASN inhibition-mediated effects that include gene expression changes and inhibition of β-catenin. Together, the results strongly support investigation of combined FASN inhibition and taxane treatment as a therapy for a variety of human cancers.

1. Introduction

Palmitate, the enzymatic product of fatty acid synthase (FASN), serves multiple essential and diverse functions within tumor cells to maintain cellular conditions that promote survival, growth, and proliferation. It provides a substrate for the anabolic synthesis of long-chain and complex cellular lipids and post-translational protein modification. Palmitate and palmitate-derived lipids function in cell metabolism, membrane architecture, protein localization, and intracellular signaling; cellular processes that are altered during oncogenic transformation and cancer progression (Gonzalez-Guerrico et al., 2016; Menendez and Lupu, 2007; Daniels et al., 2014; Flavin et al., 2010). Tumor cells have increased demand for ATP and metabolic macromolecules and must sustain survival and mitogenic signal transduction (Ward and Thompson, 2012; Vander Heiden et al., 2009), which requires lipid raft membrane microdomains densely packed with lipid-modified signaling proteins (e.g. H/N/K-Ras, EGFR, Akt) and lipid-based signaling molecules such as diacylglycerol and phosphatidylinositol (Simons and Sampaio, 2011; Lingwood and Simons, 2010; Levental et al., 2010). Whether a cause or consequence, FASN expression increases with tumor progression in many tumor types, including lung, breast, pancreatic, ovarian, colorectal, and prostate cancer (Ueda et al., 2010; Shah et al., 2006; Zaytseva et al., 2012; Witkiewicz et al., 2008; Sebastiani et al., 2006; Puig et al., 2008), and increased FASN expression associates with diminished survival and response to classical chemotherapeutic agents (Ueda et al., 2010; Tao et al., 2013; Nguyen et al., 2010; Notarnicola et al., 2012; Witkiewicz et al., 2008; Zaytseva et al., 2012). Thus, FASN presents an attractive target for the development of selective inhibitors for the treatment of cancer. Strong rationale exists for developing selective, highly active FASN inhibitors as both a single agent cancer therapy and also in combination with targeted and standard chemotherapy agents.

Abbreviations: NSCLC, Non-small-cell lung cancer; TGI, Tumor growth inhibition; MEM, Minimal essential media; DMEM, Dulbecco's modified Eagle medium; FBS, Fetal bovine serum; CS-FBS, Charcoal-filtered FBS—fetal bovine serum; IMDM, Iscove's modified Eagle medium; LC-MS, Liquid chromatography–mass spectrometry; PBS, Phosphate-buffered saline; FITC, Fluorescein isothiocyante, gene symbols and common abbreviations such as DNA and RNA are not defined.

* Corresponding author at: Cell Design Labs, Emeryville, CA, USA.
E-mail address: tim@celldesignlabs.com (T.S. Heuer).

http://dx.doi.org/10.1016/j.ebiom.2016.12.012

The rationale for use of FASN inhibitors as a key component of combination therapy derives from known cellular effects of FASN inhibition (Ventura et al., 2015; Chuang et al., 2011; Kridel, 2004; Puig et al., 2009, 2008; Tomek et al., 2011) that include (1) blockade of palmitate synthesis, (2) disruption of membrane-associated protein localization and plasma membrane architecture, (3) inhibition of oncogenic signal transduction (e.g. Wnt-beta-catenin and Akt), (4) gene expression reprogramming, and (5) induction of tumor cell apoptosis. In studies by Ventura et al. demonstrating these effects, many tumor cell lines were found to be uniquely addicted to palmitate synthesis and consequently killed by FASN inhibition. Non-tumor diploid cells such as endothelial cells or fibroblasts showed a modest decrease in proliferation but did not exhibit the cellular perturbations, for example, gene expression reprogramming, or undergo apoptosis. The disruption of membrane architecture and protein palmitoylation and localization provide direct mechanisms to sensitize tumor cells to chemotherapy or targeted agents. Altered membrane composition may facilitate entry of agents into tumor cells where they can exert their therapeutic activity while sparing non-tumor cells; for example, FASN inhibition in certain tumor cell lines changes the lipid composition of the plasma membrane, increasing the ability of doxorubicin to gain access to the cytoplasm (Rysman et al., 2010). Agents that target proteins or biological processes affected by FASN inhibition provide a further basis for designing rational combination partners. For example, agents that target palmitoylated or lipid raft-associated proteins may synergize with FASN inhibition if the localization and function of the target protein is determined by palmitoylation. Examples of palmitoylated proteins that are the known targets of approved anti-cancer therapies include tubulin and EGFR (Caron and Herwood, 2007; Caron et al., 2001; Zambito and Wolff, 1997; Ozols and Caron, 1997; Caron, 1997; Runkle et al., 2016; Bollu et al., 2015; Miura et al., 2006).

Previously, we described the characterization of the orally bioavailable, potent, and selective small molecule FASN inhibitor TVB-3166 as monotherapy in preclinical tumor models (Ventura et al., 2015). Here we report preclinical studies with TVB-3166 and the related molecule TVB-3664 that demonstrate significantly enhanced anti-tumor efficacy when FASN inhibition is combined with paclitaxel or docetaxel in vitro and in vivo. Others have studied the activity of cerulenin, an irreversible FASN inhibitor with off-target activity against many other enzymes, in combination with docetaxel in HER2-positive breast cancer cells (Menendez et al., 2004). These results provided evidence of synergistic tumor cell killing by the cerulenin–docetaxel combination; however, the significance of FASN to the findings was uncertain due to the off-target activities of cerulenin. Our studies utilized highly selective FASN inhibitors with optimized pharmacological properties, and this enabled the discovery of a mechanism-based rationale for combining FASN inhibition with taxanes that was supported by in vivo efficacy studies in varied xenograft tumor models. FASN inhibition alone inhibits tubulin palmitoylation, tubulin expression, and microtubule organization in tumor cells but not in non-tumor cells such as fibroblasts. These FASN inhibitor-mediated tumor cell effects are enhanced in combination with a taxane. Further, the combined treatment of tumor cells with FASN inhibition and a taxane increases the induction of cell killing and inhibition of cell growth in in vitro assays such as colony growth. In vivo, strongly increased inhibition of xenograft tumor growth occurs with combined TVB-3166 and taxane administration. Impressively, the effects include induction of near complete tumor regression in a variety of diverse tumor cell-line- and patient-derived tumor models that include lung, ovarian, pancreatic, and prostate tumor models. Pharmacodynamic analysis of xenograft tumors revealed enhanced inhibition of beta-catenin expression and signaling as well as a sensitization to gene expression reprogramming that occurs with FASN monotherapy in vitro. Together, these results provide compelling mechanism- and efficacy-based evidence for combined FASN and taxane therapy as a cancer therapy.

2. Materials and Methods

2.1. Protein Palmitoylation

The NSCLC tumor cell line, A549 (KRAS G12S mutant), was treated for 16 or 72 h with 20 μM 2-bromopalmitate or 50 nM TVB-3664, respectively, in Advanced formulation MEM (Thermo Fisher) supplemented with 1% charcoal-stripped FBS (CS-FBS) and 1% L-glutamine. For acyl–biotinyl exchange, cells were lysed in lysis buffer containing N-Ethylmaleimide to block free thiol groups and palmitoylation sites were labeled with biotin using the method as previously described (Wan et al., 2007) with minor modifications. Briefly, NEM-blocked lysates were treated with 1 M hydroxylamine (pH 7.4) for 1 h followed by incubation with an HPDP-biotinylation solution (pH 7.4). Protein concentrations were normalized using BCA assay. Biotinylated proteins were pulled down with Streptavidin–Agarose beads (ThermoFisher). Western blots were performed to detect palmitoylated proteins. Western blot images were captured using a LiCor Odyssey imager.

2.2. β-Tubulin Confocal Immunofluorescence

For confocal immunofluorescence imaging, 22Rv1 or MRC-5 cells were treated in Advanced formulation MEM (Thermo Fisher) supplemented with 1% charcoal-stripped FBS and 1% L-glutamine. After a 96-h compound treatment, cells were treated with microtubule stabilizing buffer (PIPES (80 mM, pH 6.8), $MgCl_2$ (1 mM), EGTA (5 mM)) supplemented with 0.5% Triton X-100 for 30 s, then fixed by overlaying 8% paraformaldehyde and incubating for 15 min at room temperature. Microtubules were labeled using anti-β-tubulin antibody (Cell Signaling) and secondary antibody conjugated to Alexa-Fluor-488 fluorescent dye (Thermo Fisher). Slides were mounted in Prolong mounting media and imaged using a Zeiss LSM 510 or Leica SP8 confocal microscope. The Leica SP8 was used with permission from Stanford University School of Medicine Cell Sciences Imaging Facility who obtained the microscope with National Center for Research Resources (NCRR) Award 1S10OD010580.

2.3. Soft Agar Colony Formation

For soft agar colony growth assays, cells were treated in an agarose matrix composed of compound treatment (DMSO, TVB-3166, taxane (paclitaxel or docetaxel), or combination), 0.35% ultrapure agarose and IMDM (ThermoFisher) supplemented with 10% fetal bovine serum, 1% non-essential amino acids, and 1% L-glutamine. The cell treatment layer was placed on a base agarose layer composed of 0.6% bactoagar and IMDM supplemented with 10% fetal bovine serum, 1% non-essential amino acids, and 1% L-glutamine. A liquid feeder layer containing compound was added on top and changed weekly. After 3–4 weeks of colony growth, cells were stained using 0.005% crystal violet and images were taken of each well.

2.4. Western Blot

For Western blot experiments, cells were treated with DMSO for 96 h in Advanced formulation MEM (ThermoFisher) supplemented with 1% charcoal-stripped FBS and 1% L-glutamine. Cells were lysed using cell lysis buffer (Cell Signaling) supplemented with phosphatase and protease inhibitors (ThermoFisher). Lysate concentrations were determined using BCA and normalized for protein load. Western blot images were captured using a LiCor Odyssey imager. For pharmacodynamic analysis of xenograft tumors, tumor lysates from individual mice in each treatment group were pooled such that each tumor contributed an equal amount of total protein to the pooled sample. Individual tumor lysates were not analyzed nor were the pooled samples analyzed multiple times; therefore, statistical significance was not determined for observed changes.

2.5. Annexin V Flow Cytometry

Cells were seeded in growth media. One day after seeding, the media was changed to the Advanced formulation MEM treatment media. Cells were treated with TVB-3166 for 24 to 96 h and harvested by Accutase (Gibco, cat. no. A11105), washed with cold PBS, and stained for Annexin V staining (FITC Annexin V Apoptosis Detection Kit II ; BD Pharmingen cat. no. 556570). Flow Cytometry analysis was performed at Stanford University's Shared FACS Facility using the LSRII·UV instrument that was obtained by Stanford University using NIH S10 Shared Instrument Grant (S10RR027431–01). Data were analyzed at 3-V Biosciences using FlowJo software (Ashland, OR).

3. Paclitaxel Concentration Determination in Cell Pellets and Supernatants

Calu-6 cells were treated with 100 nM TVB-3166 for 24 h or 50 nM TVB-3664 for 48 h. Paclitaxel was added to the cell culture media to a final concentration of 6 nM. After the 2 h of incubation with paclitaxel, cells and supernatant were collected for analysis. In the control groups, cells were not pre-treated with FASN inhibitors. Treatments were performed in Advanced formulation MEM (Thermo Fisher) supplemented with 1% charcoal-stripped FBS and 1% L-glutamine. All treatments were performed in duplicate. At the end of the incubation, cell culture media were collected into polypropylene tubes; cell pellets were resuspended in 0.5 ml of PBS, collected into the polypropylene tubes, and cells were counted. 100 μl of media or cell suspension were treated with 200 μl of acetonitrile containing the internal standard. Paclitaxel was extracted from cells and media by extensive shaking and further centrifugation. For cell supernatants, 10 μl was subjected to LC-MS-MS analysis. The concentration of paclitaxel in cell pellet and supernatant samples was measured by a quantitative LC-MS-MS method using deuterated paclitaxel as an internal standard. The method involved protein precipitation, extraction of paclitaxel and the internal standard from biological matrices, and injection of diluted extract into LC-MS-MS for paclitaxel detection. Paclitaxel and deuterium labeled paclitaxel (Paclitaxel-D5) as internal standard were obtained from Santa Cruz Biotechnology, Inc. Stock solutions of paclitaxel and IS were prepared in acetonitrile at concentrations of 1 mg/ml each. Spiking solutions of paclitaxel were prepared by appropriate dilutions with acetonitrile. HPLC or MS grade reagents were used to prepare chromatographic mobile phases. Chromatographic separations were performed by Thermo Scientific Aria LC system consisting of CTC PAL cooling auto-sampler and Agilent binary pumps. A Thermo BetaBasic-18 column (50 × 2.1 mm, 5 μM particle size) was used. Mobile phases composed of water, containing 0.1% formic acid (mobile phase A), and acetonitrile with 0.1% of formic acid (mobile phase B) were used. The elution gradient to achieve chromatographic separation was 5–95% B in 2 min, 1 min at 95% B, and 0.5 min equilibrium at 5% B. Flow rate was set at 1 ml/min. The eluted analytes were detected using an API Sciex 4000 in positive electrospray mode. A Parker–Ballston LC-MS gas generator supplied nitrogen. The paclitaxel and IS were analyzed by multiple reaction monitoring mode (MRM) with the transitions of 876.6 → 308.1 for paclitaxel, and 881.6 → 313.5 for IS. Both paclitaxel and IS were monitored as their respective most abundant adduct ions $[M + Na]^+$ to achieve better sensitivity. Data were acquired by Analyst 1.5 software. The calibration curves were established by plotting peak area ratios of paclitaxel to IS versus nominal concentration. A weighted least-squares linear regression was applied to generate a calibration curve. The calculation of paclitaxel concentrations was performed with Analyst 1.5 software.

3.1. Tumor Cell Line Xenograft Studies

Female BALB-c-nude mice were inoculated subcutaneously at the right flank with PANC-1 or OVCAR-8 tumor cells. TVB-3166 treatment via oral gavage administration was initiated when the mean tumor size reached approximately 150 mm^3. Mice were assigned into treatment groups ($N = 10$) using a randomized block design based upon their tumor volumes. Tumor sizes were measured twice weekly in two dimensions using a caliper, and the volumes were expressed in mm^3 using the formula: $V = width^2 \times length \times 0.5$. The study was terminated 6 h after the final dose. Tumor growth inhibition (TGI) was calculated as the percentage of tumor growth, relative to tumor size at the start of treatment, in drug-treated groups compared to vehicle-treated groups. The Mann–Whitney *U* test was used to assess statistical significance of the mean tumor size between drug and vehicle-treated groups. The in-life phase of the studies was conducted by Crown Biosciences (Santa Clara, CA, U.S.A., and Beijing, China). The experimenters were not blinded to group assignments.

3.2. Patient-Derived Xenograft Studies

Female BALB-c-nude mice implanted unilaterally in the flank region with tumor fragments harvested from donor animals. When tumors reached approximately 100–300 mm^3, animals were matched by tumor volume into treatment and control groups and TVB-3166 dosing by oral gavage was initiated. Tumor dimensions were measured twice weekly by digital caliper and data including individual and mean estimated tumor volumes (mean TV ± SEM) recorded for each group; tumor volume was calculated using the formula (1) $TV = width^2 \times length \times 0.52$. Tumor growth inhibition (TGI) was calculated as the percentage of tumor growth, relative to tumor size at the start of treatment, in drug-treated groups compared to vehicle-treated groups. The in-life phase of the studies were conducted by Champions Oncology (Baltimore, MD). The experimenters were not blinded to group assignments.

3.3. Animal Work Statement

CrownBio IACUC follows the “Guide of Animal Care and Use” NRC 2011, Chinese National Standard and Local government's regulations as well as animal welfare assurance number (A5896-01TC and A5895-01BJ). As an AAALAC accreditation facility, Crown Bioscience IACUC agrees to play a role as monitoring the animal activities to ensure the laws and regulations being well implemented in our facility. SoBran Inc.'s Institutional Animal Care and Use Committee has approved all animal use protocols at Champions Oncology and ensures that all protocols meet the guidelines described in the *Guide for the Care and Use of Laboratory Animals*.

4. Results

4.1. TVB-3166 and TVB-3664 Are Selective, Potent FASN Inhibitors

We discovered a series of selective, potent, and highly bioavailable FASN inhibitors that included TVB-3166 and TVB-3664 (Table 1, Fig. 1). TVB-3166 was evaluated in a diverse set of in vitro and in vivo studies that demonstrated the effect of FASN inhibition on palmitate synthesis, cell signaling, cell survival, gene expression, and in vivo xenograft tumor growth (Ventura et al., 2015). In these previous studies, controls with a high concentration of exogenous palmitate in the cell culture media were included; they showed that the effect of TVB-3166 on cell viability was an on-target activity of FASN inhibition. This conclusion was further supported by the observed dose–response relationship between drug treatment and the measured effect in all assays. TVB-3664 exhibits 8- to 10-fold greater potency against human and mouse FASN than TVB-3166 while retaining very high chemical similarity (Table 1). Both of these FASN inhibitors have excellent bioavailability and pharmacokinetic properties in mice that enable in vivo pharmacology and tumor growth inhibition studies (TVB-3664 data shown in Fig. 1B). TVB-3166 and TVB-3664 were used interchangeably in the studies reported here. Several tumor cell lines were used in the in vitro and in vivo studies (Table S1). FASN expression was similar

Table 1
In vitro FASN inhibition in human and mouse cells.

FASN IC_{50} (μM)	TVB-3166	TVB-3664
Human cell palmitate synthesis	0.0702	0.018
Mouse cell palmitate synthesis	0.857	0.012

across the tumor cell lines. The prostate-tumor-derived cell line 22Rv1 had the highest FASN protein expression. Requirements for some individual studies made using a particular cell line throughout the different studies difficult or impossible. Additionally, varied models were used to show the diversity of tumor types that respond to FASN inhibition.

4.2. FASN Inhibition Inhibits Tubulin Palmitoylation and mRNA Expression

Many proteins including a subpopulation of alpha- and beta-tubulin in microtubules are modified post-translationally by the addition of a palmitate moiety to cysteine side chains (Zambito and Wolff, 1997; Ozols and Caron, 1997; Caron, 1997). This modification often leads to targeting proteins to lipid raft microdomains of the plasma membrane and may serve to anchor microtubules to specific cell membranes. To examine the effect of FASN inhibition on palmitoylation of tubulin proteins, several different non-small-cell lung cancer cell lines were found to perform well in this assay and were analyzed for palmitoylation using an acyl–biotin exchange process followed by Western blotting. The procedure was validated using 2-bromopalmitate (2-BP), a substrate-based inhibitor of protein palmitoylation. Treatment of KRAS-mutant A549 tumor cells with 20 μM 2-BP for 18 h decreased levels of palmitoyl-α- and β-tubulin 27% and 79%, respectively (Fig. 2A). Comparable results were observed in A427 and CALU-6 KRAS-mutant NSCLC tumor cell lines. We then determined the effect of FASN inhibition on tubulin palmitoylation by treating cells with TVB-3664. TVB-3664 inhibits cellular palmitate synthesis with an IC_{50} value of 9 nM (Table 1). A549 cells treated with 50 nM TVB-3664 for 72 h showed a 67% and 92% loss of palmitoyl-α- and β-tubulin, respectively (Fig. 2A). The KRAS wild-type NSCLC cell line NCI-H520 showed 27% and 65% inhibition of palmitoyl-α- and β-tubulin, respectively. These results were in excellent agreement with the effects of 2-BP treatment and clearly demonstrated that FASN inhibition decreases palmitoylation of both α- and β-tubulin. FASN inhibition has been shown to reprogram gene expression, affecting many different types of genes in tumor cells including those that function in metabolism and regulation of cell growth, proliferation, and signaling (Ventura et al., 2015). Beta-tubulin expression was determined in 22Rv1 and additional tumor cell lines by RNA sequencing and quantitative RT-PCR assays. Treating cells with 1 μM TVB-3166 for 48 h decreased β-tubulin expression significantly compared to DMSO treatment. Treatment with paclitaxel alone had no effect on β-tubulin expression. The combination of TVB-3166 and paclitaxel decreased expression comparable to that observed with FASN inhibition alone (Fig. 1C). Comparable results were obtained in additional tumor cell lines including CALU-6 (non-small-cell lung) (Ventura et al., 2015). Taken together, the changes to tubulin gene expression and post-translational modification of the protein induced by FASN inhibition suggest that FASN inhibition combined with another drug-targeting microtubule function, for example, with taxane treatment, may inhibit tumor cell growth with greater efficacy. Consistent with this hypothesis, β-tubulin mRNA expression remains suppressed in the presence of combined TVB-3166 and paclitaxel treatment (Fig. 1C).

4.3. FASN Inhibition Disrupts Microtubule Organization

To investigate the effect of FASN inhibition on cellular microtubule organization, tumor cells were stained with an immuno-fluorescent antibody against β-tubulin following 96 h of treatment with vehicle (DMSO), TVB-3166, paclitaxel, or the combination of TVB-3166 and

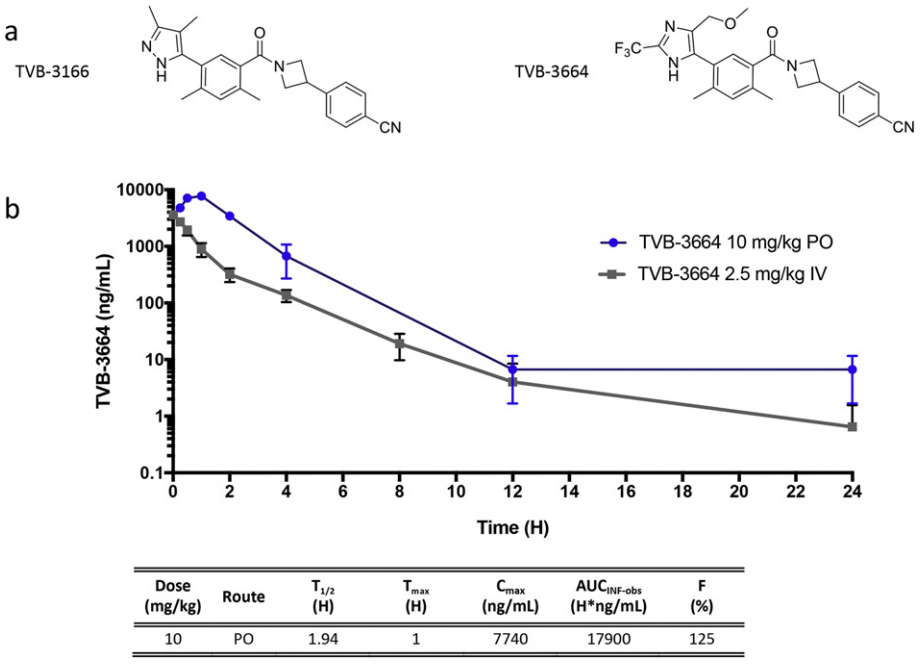

Dose (mg/kg)	Route	$T_{1/2}$ (H)	T_{max} (H)	C_{max} (ng/mL)	$AUC_{INF-obs}$ (H*ng/mL)	F (%)
10	PO	1.94	1	7740	17900	125

Fig. 1. TVB-3166 and TVB-3664 small molecule FASN inhibitors. (A) Chemical structure of TVB-3166 and TVB-3664. (B) Pharmacokinetic analysis of TVB-3664 in mice. Drug levels were determined from 3 different mice for each time point following administration by oral gavage or intravenous injection. (Bayside Biosciences, San Jose, CA). For oral dosing, TVB-3664 was formulated at 3-V Biosciences in 100% PEG-400 and diluted with water to a final PEG concentration of 30% immediately before dosing. For iv dosing TVB-3664 was formulated Bioanalytical analysis was performed at 3-V Biosciences by mass spectrometry.

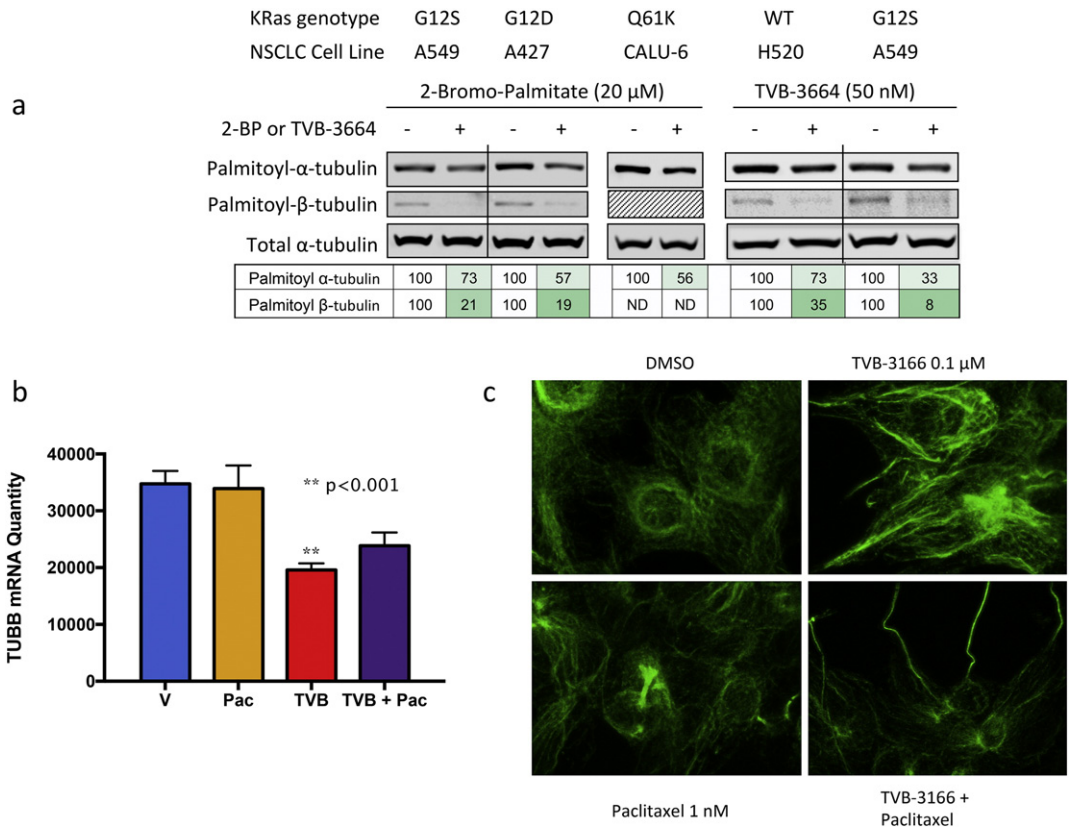

Fig. 2. FASN inhibition disrupts tubulin palmitoylation, expression and microtubule organization. (A) TVB-3664 inhibits tubulin palmitoylation in NSCLC cell lines. Cells were treated with DMSO, TVB-3664 (48 h), or 2-bromopalimitate (18 h) as a positive control as indicated. Cell lysates were harvested and analyzed for palmitoylation of alpha-or beta-tubulin using acyl-biotin exchange chemistry followed by Western blot analysis. (B) TVB-3166 inhibits b-tubulin mRNA expression. 22Rv1 prostate tumor cells were treated with DMSO, TVB-3166, paclitaxel, or the combination of TVB-3166 and paclitaxel for 48 h in vitro. Three individual biological replicates were treated and used for analysis by RNA sequencing to quantitate mRNA levels. TVB-3166-treated cells showed a significant decrease in b-tubulin mRNA ($p < 0.001$) compared to vehicle or paclitaxel-treated cells. Combination-treated cells also showed decreased b-tubulin expression. (C) FASN inhibition disrupts tumor cell microtubule organization. 22Rv1 prostate tumor cells were treated with DMSO, TVB-3166, paclitaxel, or the combination of TVB-3166 and paclitaxel for 96 h. Microtubule organization was visualized by immuno-fluorescence microscopy using an anti-b-tubulin antibody. Similar effects were observed with TVB-3664 in place of TVB-3166 or docetaxel in place of paclitaxel (Fig. S1). Non-tumor cells (MRC-5 lung fibroblasts) were not affected significantly by TVB-3664 and paclitaxel or docetaxel treatment (Fig. S1).

paclitaxel. 22Rv1 prostate tumor cells were found to have optimal features for this study including cell size, morphology, and preservation of microtubule structure following cell fixation. The results shown are representative of 3 separate biological replicate experiments. In vehicle-treated cells, an organized microtubule structure was observed (Fig. 1D). A ring-like structure was seen outside of the nucleus with lightly staining filaments dispersed throughout the cell. FASN inhibition with TVB-3166 caused microtubule strands to appear longer and more intensely stained than observed in vehicle- or paclitaxel-treated cells and the ring-like structure was not apparent. In paclitaxel-treated cells, the overall organization of tubulin was similar to vehicle-treated cells with the presence of mitotic-arrested cells as expected. Combined treatment with TVB-3166 and paclitaxel induced further changes than observed with TVB-3166 single agent treatment; combination treatment caused tubulin strands to appear very long and thin with major disruption of the normal organization. 22Rv1 tumor cells treated with TVB-3664 or the combination of TVB-3664 and docetaxel showed the same results as cells treated with TVB-3166 or TVB-3166 plus paclitaxel (Fig. S1), demonstrating that FASN inhibition combined with different taxane molecules used for the clinical treatment of cancer induce the same effects in this in vitro assay.

4.4. Combined FASN Inhibition and Taxane Treatment Increases in Vitro Tumor Cell Growth Inhibition

The effect of FASN inhibition and taxane treatment on tumor cell growth was investigated using soft agar colony growth assays. Treatment of 22Rv1 prostate tumor and CALU6 non-small-cell lung tumor cell lines with 0.1 μM TVB-3166 reduced both colony number and size in a 3- to 4-week growth assay (Fig. 3A). Paclitaxel treatment at 0.3 or 1.0 nM did not affect colony size or number; however, 3 nM paclitaxel showed strong inhibition of colony growth of both tumor cell lines. The combined treatment of 0.1 μM TVB-3166 and 1 nM paclitaxel showed greater inhibition of colony growth than either agent alone at these concentrations. Increasing the paclitaxel concentration to 3 nM combined with 0.1 μM TVB-3166 inhibited colony growth completely or nearly completely in CALU6 and 22Rv1 cells, respectively. Because 3 nM paclitaxel did not inhibit colony growth completely as a single agent in 22Rv1 cells, increased growth inhibition compared to single agent FASN or taxane treatment was discernable with the combination of 0.1 μM TVB-3166 and 3 nM paclitaxel in these cells. Three independent biological replicate experiments were performed with the 22Rv1 cells using paclitaxel twice (representative data in Fig. 2A) and docetaxel once (Fig. S2). Comparable results were obtained with paclitaxel and docetaxel. A single experiment with the CALU-6 tumor cell lines was performed to confirm the results in a different tumor cell type.

4.5. FASN Inhibition Does Not Affect Intracellular Paclitaxel Concentration

The possibility that the mechanism of action for FASN and taxane combination activity results from an increased intracellular paclitaxel concentration as a result of FASN inhibition was examined by treating tumor cells with vehicle (DMSO), TVB-3166 (0.1 μM), or TVB-3664 (0.05 μM) for 24 or 48 h followed by the addition of 6 nM paclitaxel

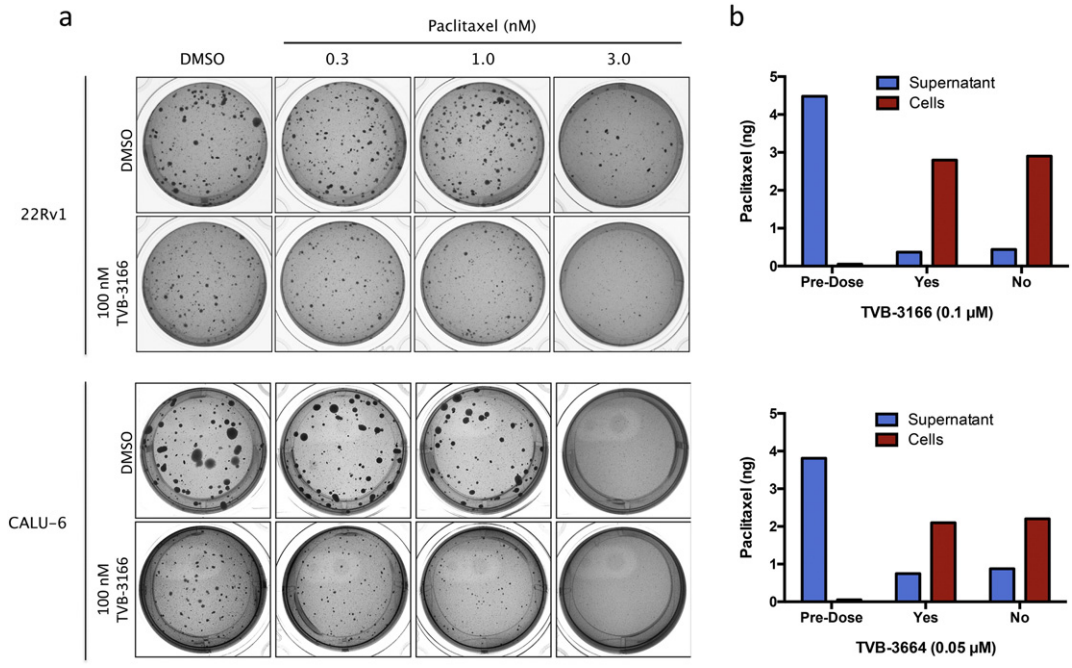

Fig. 3. Combined treatment of tumor cells with TVB-3166 and paclitaxel in vitro increases soft agar colony growth inhibition and induction of apoptosis. (A) 22Rv1 prostate tumor cells (top panel) or CALU-6 NSCLC cells (bottom panel) were treated with a dose–response matrix of TVB-3166 and paclitaxel. 22Rv1 and CALU-6 tumor cells treated with 0.1 μM TVB-3166 and 0.001 μM paclitaxel showed increased inhibition of colony growth compared to treatment with each agent alone. Colony growth was inhibited completely with 0.1 μM TVB-3166 and 0.003 μM paclitaxel. (B) Intracellular paclitaxel concentration in CALU-6 tumor cells is unaffected by FASN inhibition. CALU-6 tumor cells were treated with DMSO, TVB-3166, or TVB-3664 for 24 (A) or 48 (B) hours. Cell lysates and supernatants were collected and the paclitaxel concentration in each matrix was determined by precipitation, extraction, and LC-MS-MS.

for 2 h. The intracellular paclitaxel concentration determined by mass spectrometry was unchanged by TVB-3166 or TVB-3664 treatment (Fig. 3B; Table 3). The results shown for TVB-3166 are representative of two independent experiments. A single experiment with TVB-3664 was performed to confirm the results with TVB-3166. Therefore, the enhanced anti-tumor activity of FASN inhibition and taxane treatment is not the result of an increased intracellular taxane concentration.

4.6. Combined FASN Inhibition and Taxane Treatment Strongly Inhibit Xenograft Tumor Growth and Induce Tumor Regression in Tumor Models from Different Tumor Types

The anti-tumor efficacy of combining FASN inhibition and taxane treatment was determined in studies with several murine xenograft tumor models representing non-small-cell lung, ovarian, prostate, and pancreatic tumor types (Table 4). Non-small-cell lung xenograft tumor models included KRAS-mutant tumor cell lines (CALU6 and A549) and CTG-0165_P + 6, a patient-derived tumor with wild-type KRAS and EGFR (Fig. 4). CTG-0165_P + 6 is a tumor that is related to the CTG-0165 tumor reported previously (Ventura et al., 2015). The current study uses the tumor following 6 passages in mice. During these passages, the growth characteristics and the response to single agent TVB-3166 treatment changed. In these three studies with 10 mice per treatment group, single agent TVB-3166 did not inhibit tumor growth significantly. Single agent paclitaxel exhibited 48–63% tumor growth inhibition. Both paclitaxel and docetaxel were investigated in the A549 xenograft study and demonstrated comparable single agent activity (48% and 52%, respectively). The combination of TVB-3166 and paclitaxel resulted in tumor regression in the CALU6 and CTG-0165_P + 6 patient-derived tumor models. In the A549 tumor model, TVB-3166 combined with paclitaxel or docetaxel to inhibit tumor growth 76% and 81%, respectively. Thus, in each of the three lung tumor xenografts, the anti-tumor efficacy was significantly enhanced in the FASN and taxane combination treatment groups compared to single agent dosing (Table 2). In the CALU-6 and CTG-0165_P + 6 models, significant tumor regression was observed with the combination treatment. Analysis of plasma and tumor concentrations of TVB-3166 6 h after final dosing showed that drug levels in the combination and single agent groups were comparable (Table 2). Paclitaxel or docetaxel concentrations 6 h after final dosing often were below the limit of quantitation or not possible to analyze due small tumor size.

Ovarian (OVCAR8), prostate (22Rv1), and pancreatic (PANC1) xenograft tumor models were investigated as well. Results similar to those observed in the NSCLC xenograft tumor models were found (Fig. 5). In each of these three different tumor models, the combination treatment group exhibited significantly improved anti-tumor efficacy compared to single agent TVB-3166 or paclitaxel treatment; combination FASN and taxane treatment resulted in tumor growth inhibition (TGI) values of 130%, 97%, and 88% in the OVCAR8, 22Rv1, and PANC1 tumor xenografts, respectively. The OVCAR8 tumor model differed from the others in that significant single agent TVB-3166 activity was observed: 59% and 74% TGI for 60 mg/kg and 100 mg/kg doses, respectively. Single-agent paclitaxel TGI values were 83%, 57%, and 56% in the OVCAR8, 22Rv1, and PANC1 tumor xenografts, respectively. Together, the results from these 6 xenograft tumor models representing diverse tumor types provide compelling evidence of significantly enhanced tumor growth inhibition by the combination of FASN inhibition and taxane treatment. Combined administration of these agents caused strong tumor growth inhibition in all tumor types (>81%TGI) and tumor regression was observed in 3 of 6 tumor models.

4.7. Combined FASN Inhibition and Taxane Treatment Sensitize Xenograft Tumors to Gene Expression Changes Associated with in Vitro FASN Inhibition

FASN inhibition is associated with extensive changes in tumor cell gene expression in vitro with effects on genes that function in metabolism, proliferation and survival (Ventura et al., 2015). Analysis of the

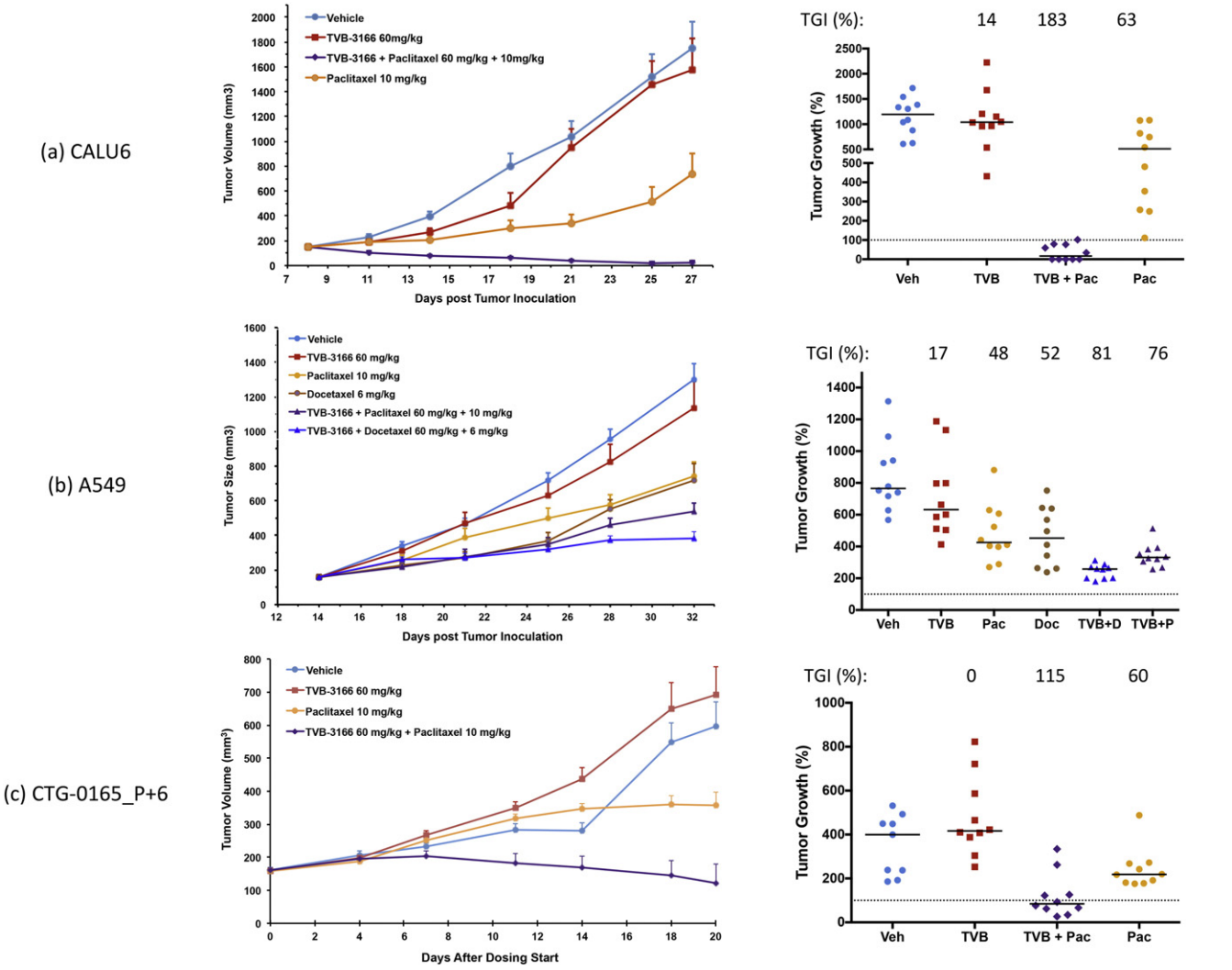

Fig. 4. Combined treatment of NSCLC tumor xenografts with TVB-3166 and a taxane (paclitaxel or docetaxel) inhibits tumor growth synergistically compared to single agent activity. A minimum of 10 mice per treatment group was used in all studies. (A) CALU6 NSCLC adenocarcinoma cell line. (B) A549 NSCLC adenocarcinoma cell line. (C) CTG-0165_P + 6 NSCLC adenocarcinoma patient-derived tumor. TVB-3166 was dosed once daily by oral gavage at 60 mg/kg. Paclitaxel was dosed once every 4 days by intravenous administration at 10 mg/kg. Docetaxel was dosed once every 7 days by intravenous administration at 8 or 6 mg/kg. In groups dosed with both TVB-3166 (60 mg/kg) and paclitaxel (10 mg/kg) or docetaxel (8 or 6 mg/kg), TVB-3166 was administered 2 h before taxane administration. Animals were randomized according to tumor size and drug treatment was started when the mean tumor size was 150–200 mm^3. Tumors and blood samples were harvested 2 h after the last dose. TVB-3166 and paclitaxel plasma and tumor drug concentrations were determined by mass spectrometry. The in-life phase for the CALU-6 (A) and A549 (B) studies was performed at Crown Biosciences (Santa Clara, CA; Beijing, China). The in-life phase for the CTG-0165_P + 6 study (C) was performed at Champions Oncology (Baltimore, MD).

patient-derived NSCLC tumor CTG-0165 by whole-genome RNA sequencing revealed many of these same changes in xenograft tumors treated with 60 mg/kg TVB-3166 combined with 10 mg/kg paclitaxel but not in tumors treated with either drug alone (Fig. 6A). Tumors treated with single agent TVB-3166 at 60 mg/kg once daily had a gene expression profile that was similar to tumors from vehicle-treated mice. Similarly, paclitaxel did not affect gene expression significantly. From these data, it appears, paclitaxel treatment sensitized xenograft tumors to gene expression changes associated with FASN inhibition.

Table 2
TVB-3664 mouse PK parameters.

Dose (mg/kg)	Route	$T_{1/2}$ (H)	T_{max} (H)	C_{max} (ng/ml)	$AUC_{INF\text{-}obs}$ (H*ng/ml)	F (%)
10	PO	1.94	1	7740	17,900	125

4.8. Combined FASN Inhibition and Taxane Treatment Inhibits β-Catenin Expression and Phosphorylation Associated with Activation

Pharmacodynamic analysis of A549 tumor samples collected 2 h after final dose administration on day 20 showed inhibition of both

Table 3
Paclitaxel quantitation in CALU-6 NSCLC cells before and after FASN inhibition.

		Paclitaxel (ng)	
Treatment	Time (H)	Cells	Supernatant
None	0	0	3.81
50 nM TVB-3664	48	2.20	0.876
DMSO	48	2.10	0.749
None	0	0	4.48
100 nM TVB-3166	24	2.78	0.37
DMSO	24	2.94	0.44

Table 4
Tumor growth inhibition and statistical analysis of treatment groups.

Tumor model	Treatment	TGI vs. vehicle (%)	*p* value (TGI)	Plasma TVB-3166 (ng/ml)[1]	Tumor TVB-3166 (ng/g)[1]
CALU-6	TVB-3166	14	0.7207	6799	5006
	TVB-3166 + P	183[2]	<0.0001	8651	4628
	Paclitaxel (P)	63	0.0012	—	—
	Vehicle	—	1.000	—	—
A549	TVB-3166	17	0.2443	9542	—
	TVB-3166 + P	76[3]	<0.0001	10362	—
	TVB-3166 + D	81[4]	<0.0001	6218	—
	Paclitaxel (P)	48	0.0011	—	—
	Docetaxel (D)	52	0.0011	—	—
	Vehicle	—	1.000	—	—
CTG-0165_P + 6	TVB-3166	0	0.2110	4150	—
	TVB-3166 + P	115[5]	0.0015	2372	—
	Paclitaxel (P)	60	0.0947	—	—
	Vehicle	—	1.000	—	—

[1] 6 h post last dose.
[2] TVB-3166 + paclitaxel vs. paclitaxel TGI: $p < 0.0001$.
[3] TVB-3166 + paclitaxel vs. paclitaxel TGI: $p < 0.0032$.
[4] TVB-3166 + paclitaxel vs. docetaxel TGI: $p < 0.0052$.
[5] TVB-3166 + paclitaxel vs. pacltaxel TGI: $p < 0.0015$.

total β-catenin expression and S675 phosphorylation in tumors from the combination treatment group (Fig. 6B). Inhibition of Akt signaling (S473 phosphorylation) was not observed. Phosphorylation of β-catenin at S675 is associated with nuclear localization and β-catenin activity. Tumors collected from the paclitaxel or docetaxel combination treatment groups showed 44% and 38% inhibition of β-catenin S675 phosphorylation, respectively. Slight inhibition (25%) of S675 phosphorylation was detected in docetaxel treated tumors. Total β-catenin expression and S675 phosphorylation levels were comparable to vehicle-treated levels in tumor samples from groups treated with single agent TVB-3166 or paclitaxel. Myc expression was measured as a downstream marker for b-catenin activity. Myc expression was below a level that could be reliably detected and quantitated in the A549 xenograft tumors; however, it appeared to be detected at a very low level in vehicle and single agent treatment groups while undetectable in the TVB-3166 + paclitaxel treatment group. Statistical significance was not determined for the observed changes.

5. Discussion

Combined FASN inhibition and taxane treatment demonstrated significantly enhanced anti-tumor efficacy in diverse xenograft tumor models from lung, ovarian, prostate, and pancreatic cancers compared to single agent therapy. This was observed in 6 of 6 xenograft efficacy studies, and in 3 of 6 studies, combination treatment caused tumor regression, which was not observed with single-agent treatment in any of the tumor models. Previous in vitro and in vivo studies with TVB-3166 supported investigating several different tumor types and also suggested a focused study of KRAS mutant non-small-cell lung tumor models (Ventura et al., 2015). TVB-3166 belongs to a series of proprietary FASN inhibitors with high chemical similarity. TVB-2640, the lead molecule in this series of inhibitors, is completing Phase I clinical development for the treatment of solid tumors, where it demonstrated excellent oral bioavailability and pharmacokinetics that translated into sustained target inhibition and highly promising signs of clinical efficacy at well-tolerated doses (Dean et al., 2016). TVB-2640 clinical development is investigating both monotherapy and combination therapy administration with taxane therapies such as paclitaxel. Our current studies investigated two cell-line-derived and one patient-derived lung tumor xenograft models and significant tumor regression was induced by combination treatment in 2 of these 3 models. The results also demonstrated that significantly improved efficacy occurs when FASN inhibition is combined with either paclitaxel or docetaxel, supporting a model that the mechanism of additivity or synergy is linked directly to the FASN and taxane mechanisms of action. A scientific rationale and model for the enhanced activity observed with the drug combination was developed from cell biology studies (Fig. 7). This model incorporates findings from the current studies and from previously reported studies showing that single-agent FASN inhibition with TVB-3166 induces apoptosis in tumor cells by remodeling cell membranes and disrupting localization of lipid raft-associated proteins, inhibiting signaling pathways that include Akt and beta-catenin, and reprogramming gene expression (Ventura et al., 2015).

Alpha and beta-tubulin are palmitoylated (Caron and Herwood, 2007; Caron et al., 2001; Zambito and Wolff, 1997; Ozols and Caron, 1997; Caron, 1997), and tubulin palmitoylation helps to anchor microtubule filaments in the plasma membrane and supports functions needed for cellular transport and division. Inhibition of FASN was shown to decrease tubulin palmitoylation leading to profound disruption of microtubule organization in tumor cells. Notably, non-tumor cells such as MRC5 fibroblasts showed very little effect upon treatment with TVB-3664, paclitaxel, or the combination of TVB-3664 and paclitaxel (Fig. S1A-B), suggesting that combined FASN inhibition and taxane treatment will not increase toxicity to non-tumor cells and thus provide a therapeutic index for anti-tumor efficacy. Non-tumor cells including MRC5 fibroblasts and HUVEC endothelial cells have significantly higher levels of saturated fatty acids than tumor cells before and after 96 h of FASN inhibition (Fig. S1C), and this likely plays a significant role in the low sensitivity of non-tumor cells to FASN inhibition. In addition, beta-tubulin mRNA levels were decreased in tumor cells following FASN inhibition. An apparent contrast was observed between the decreased level of TUBB mRNA and increased beta-tubulin immunofluorescence staining following treatment with single-agent treatment with TVB-3166. This may be accounted for by time-dependent differences in the two assays and, additionally or alternatively, may be explained by greater quantitative accuracy of the mRNA assay or translational regulation that causes a disconnect between mRNA and protein levels. Taken together, the results provide evidence that depletion of palmitate in tumor cells fundamentally alters the function and expression of the taxane target protein (Tubulin) and cellular component (microtubules). It seems highly plausible that these mechanistic effects create a foundation for FASN inhibition and taxane treatment to act with additivity or synergy as an anti-tumor therapeutic.

Because FASN inhibition and the resulting palmitate depletion alters lipid composition of the plasma membrane and the architecture of membrane-associated proteins (Ventura et al., 2015; Marien et al., 2015), it was possible that FASN inhibition could enhance taxane activity by increasing intracellular concentration of the drug. This potential mechanism was investigated by in vitro studies that determined the intracellular paclitaxel concentration with and without FASN inhibition with TVB-3166 or TVB-3664. The results showed that FASN inhibition for 24 or 48 h did not affect the cellular paclitaxel concentration and supported a model where the enhanced anti-tumor activity of the FASN and taxane drug combination is derived from effects of FASN inhibition on tubulin palmitoylation, gene expression, and microtubule architecture.

Possible complementary or alternative mechanisms for the increased efficacy of the FASN and taxane combination therapy include effects from suppressing palmitoylation of additional proteins known to be modified by palmitate such as KRas, NRas, EGFR, Akt, Cav1, and Wnt (Yeste-Velasco et al., 2015; Bollu et al., 2015; Song et al., 2013; Eisenberg et al., 2013; Levental et al., 2010; Martin and Cravatt, 2009; Fiorentino et al., 2008), and the subsequent sensitization to taxane treatment from the inhibition of signaling through these pathways. Previous studies by many groups have shown that FASN overexpression or inhibition modulates Akt as well as other drivers of oncogenic signaling

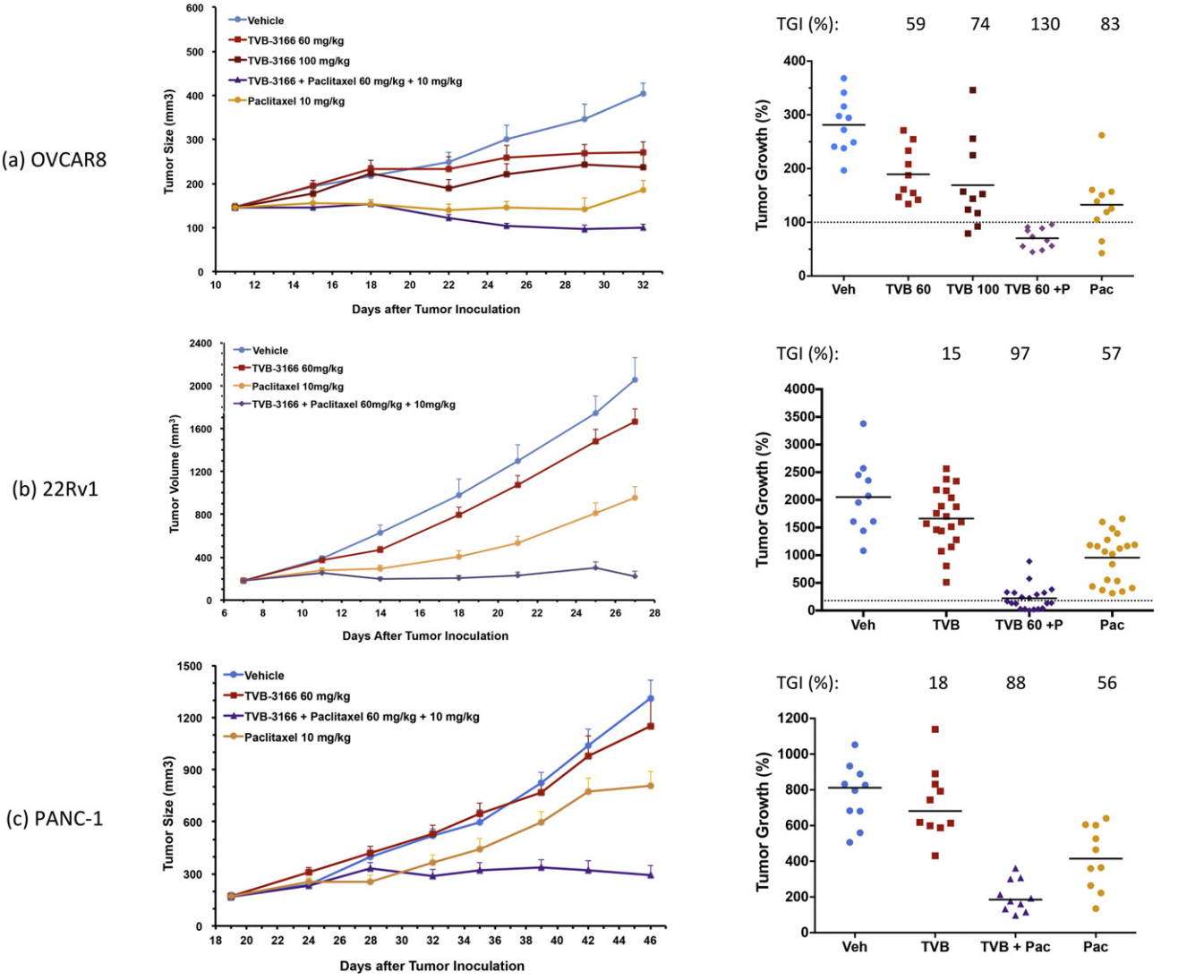

Fig. 5. Combined treatment of ovarian, prostate, and pancreatic tumor xenografts with TVB-3166 and paclitaxel inhibits tumor growth synergistically compared to single agent activity. A minimum of 10 mice per treatment group was used in all studies. (A) OVCAR8 ovarian adenocarcinoma cell line. (B) 22Rv1 castration-resistant prostate tumor cell line. (C) PANC1 pancreatic ductal adenocarcinoma tumor cell line. TVB-3166 was dosed once daily by oral gavage at 60 or 100 mg/kg. Paclitaxel was dosed once every 4 days by intravenous administration at 10 mg/kg. In groups dosed with both TVB-3166 (60 mg/kg) and paclitaxel (10 mg/kg), TVB-3166 was administered 2 h before taxane administration. Animals were randomized according to tumor size and drug treatment was started when the mean tumor size was 150–200 mm^3. Tumors and blood samples were harvested 2 h after the last dose. TVB-3166 and paclitaxel plasma and tumor drug concentrations were determined by mass spectrometry. The in-life phase for these studies was performed at Crown Biosciences (Santa Clara, CA; Beijing, China).

that include c-Met, ERBB2, EGFR, and Wnt-b-catenin (Ventura et al., 2015; Coleman et al., 2009; Uddin et al., 2010; Hu et al., 2016; Puig et al., 2011; Vazquez-Martin et al., 2008; Bollu et al., 2015). Our observation that combining TVB-3166 or TVB-3664 with taxane treatment increased efficacy in several tumor models of diverse origin and genetic features suggests the primary mechanism is fundamental to tumor cell biology and the taxane mechanism of action such as tubulin palmitoylation, expression, and the disruption of microtubule function; however, complementary mechanism may play an important role in a manner that is dependent upon tumor type. Additionally, taxane treatment may sensitize tumor cells to the effects of FASN inhibition on oncogenic signaling and/or tumor cell energetics and metabolism.

The mechanism of enhanced anti-tumor activity of the FASN and taxane drug combination in our studies includes sensitization of tumor cells to FASN inhibition-mediated gene expression changes and inhibition of beta-catenin signaling but not Akt signaling. It remains possible that sensitization to Akt inhibition or other pathways that promote tumor growth, proliferation, and survival could occur in different tumor models than those used in our studies. In vitro FASN inhibition causes these effects on gene expression and signal transduction; however, this has been observed less commonly with in vivo xenograft tumor studies by us and others. Various models have rationalized these results, finding limited or loss of effect to of FASN or SCD inhibition in in vivo studies or in vitro with rich media sources (Daniels et al., 2014; Smans et al., 2014; Peck et al., 2016; Schug et al., 2015). The explanations focus around tumor cells possessing a capacity to compensate for inhibition of lipid synthesis by reprogramming cellular metabolism and/or by the acquisition of essential lipids from the extracellular environment. The existence and importance of so-called privileged pools of intracellular palmitate and complex lipids, derived solely from de novo lipogenesis, remains an important component of tumor or diseased cell biology to elucidate more fully (Jensen-Urstad et al., 2013). Our results,

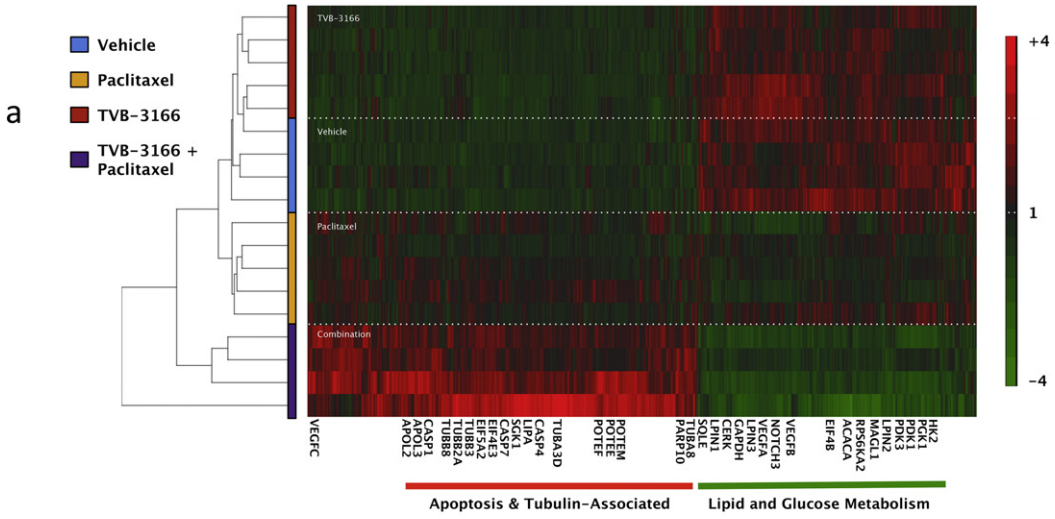

b

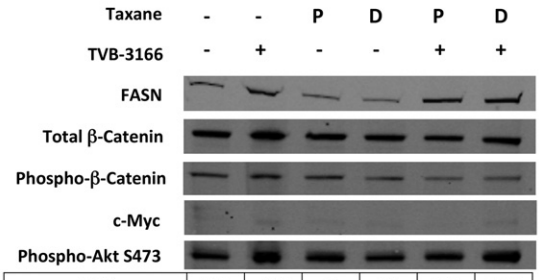

FASN	100	176	91	74	218	312
Total b-catenin	100	109	98	93	71	90
Phospho-b-Catenin	100	95	105	75	56	62
Phospho-Akt-S473	100	100	117	135	107	141

Fig. 6. Combined treatment of xenograft tumors with TVB-3166 and paclitaxel enhances pharmacodynamic effects of FASN inhibition to induce (A) gene expression changes similar to that observed in in vitro cell treatments with single-agent FASN inhibition and (B) inhibition of beta-catenin expression and phosphorylation similar to effects observed in in vitro cell treatments with single-agent FASN inhibition. Xenograft tumors were harvested 2 h following the last dose of TVB-3166 and/or taxane. For gene expression analysis, tumor pieces were preserved in RNAlater. RNA isolation was performed at 3-V Biosciences and mRNA changes were determined using RNA sequencing (RNASeq-25, Illumina, Inc). For Western blot analysis, tumor pieces were flash frozen. Tumor lysates were prepared at 3-V Biosciences in a buffer containing protease and phosphatase inhibitors.

which show that pharmacodynamic and efficacy hallmarks of in vitro FASN inhibition were recapitulated using in vivo tumor xenografts (without modification to diet or feeding schedule) when FASN inhibition is combined with taxane treatment, argue that taxane activity constrains tumor cell biological and metabolic plasticity in a way that can mimic the conditions generated by growing tumor cells under controlled serum conditions in vitro. The data reported here taken together suggest that the combined action of a selective, potent, pharmacologically optimized FASN inhibitor and taxane treatment offers broad therapeutic potential for the treatment of many types of cancer. If additional chemotherapy or targeted therapy agents with distinct mechanisms of action limit oncogenic adaptation to depletion of de novo synthesized palmitate in an effectively similar manner, optimized FASN inhibitors could provide an additive or synergistic combination partner to many existing or developmental anti-cancer drugs.

In summary, we report results demonstrating strongly enhanced inhibition of in vivo tumor xenograft growth with combined FASN inhibition and taxane treatment across a diverse set of tumor models that includes non-small-cell lung, ovarian, prostate, and pancreatic tumors. Importantly, our findings provide a strong mechanistic rationale derived from both FASN and taxane mechanisms of action for this observed increase in efficacy with the drug combination. The reported findings support a hypothesis that pharmacologically optimized FASN inhibitors can combine with a variety of anti-cancer agents from different mechanistic classes to enable significant advancement our treatment options for human cancer.

Supplementary data to this article can be found online at http://dx.doi.org/10.1016/j.ebiom.2016.12.012.

Funding

All studies were funded privately by 3-V Biosciences.

Conflicts of Interest

All authors were employees of 3-V Biosciences at the time of study execution.

Author Contributions

Timothy Heuer—study direction, data interpretation, figure composition, and writing; Richard Ventura—experiment design, data collection, data analysis, data interpretation; Kasia Mordec—experiment design, data collection, data analysis, data interpretation; Juie Lai—data collection; Marina Fridlib—data collection, data analysis; Douglas Buckley—study direction; George Kemble—study direction.

Acknowledgments

We thank Jia Li and Guanping Mao at Crown Biosciences. We thank Marie O'Farrell, Claudia Rubio, Allan Wagman, and Greg Duke at 3-V Biosciences for scientific discussions.

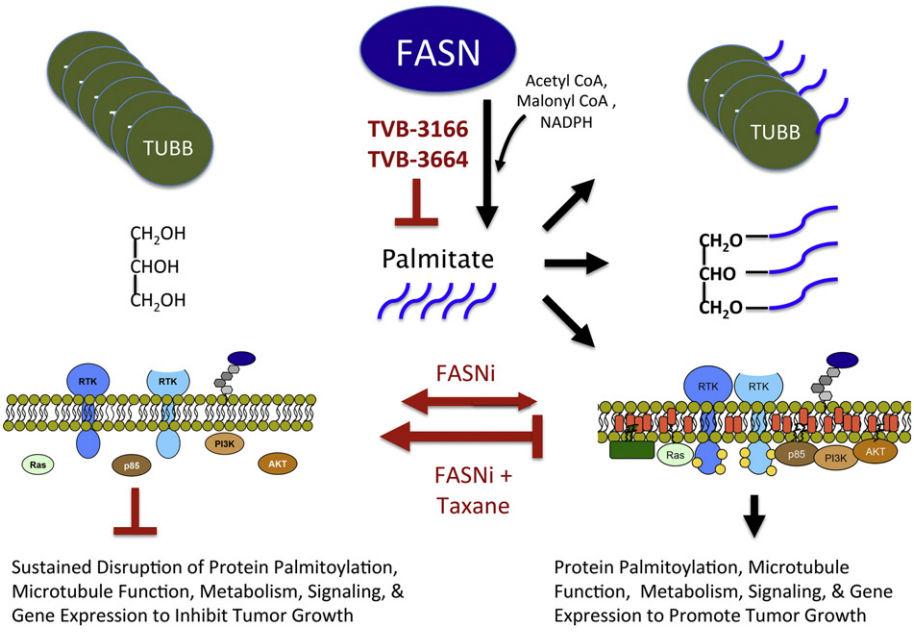

Fig. 7. Model describing the mechanism of increased anti-tumor efficacy with combined FASN inhibition and taxane treatment compared to single-agent treatment. Right panel: cellular palmitate synthesized by FASN is utilized for many cellular functions that include (1) post-translational modification of proteins including alpha- and beta-tubulin, (2) synthesis of complex lipids required for cellular metabolism and energy storage, and (3) maintenance of plasma membrane architecture to support oncogenic signaling (Ventura et al., 2015). Left panel: inhibition of FASN causes a loss of tubulin palmitoylation, depletes lipid stores that maintain tumor cell metabolism, and disrupts the plasma membrane architecture necessary for oncogenic signaling. Diminished tubulin palmitoylation and expression and altered microtubule organization sensitize tumor cells to taxane activity. Taxane activity limits the capacity of a tumor cell to adapt to FASN inhibition and causes sustained disruption of biological processes that utilize palmitate, perhaps interfering with the ability of tumor cells to acquire palmitate exogenously or utilize palmitate that is not synthesized de novo by the tumor cell.

References

Bollu, L.R., Katreddy, R.R., Blessing, A.M., Pham, N., Zheng, B., Wu, X., Weihua, Z., 2015. Intracellular activation of EGFR by fatty acid synthase dependent palmitoylation. Oncotarget 6, 34992–35003.

Caron, J.M., 1997. Posttranslational modification of tubulin by palmitoylation: I. In vivo and cell-free studies. Mol. Biol. Cell 8, 621–636.

Caron, J.M., Herwood, M., 2007. Vinblastine, a chemotherapeutic drug, inhibits palmitoylation of tubulin in human leukemic lymphocytes. Chemotherapy 53, 51–58.

Caron, J.M., Vega, L.R., Fleming, J., Bishop, R., Solomon, F., 2001. Single site alpha-tubulin mutation affects astral microtubules and nuclear positioning during anaphase in *Saccharomyces cerevisiae*: possible role for palmitoylation of alpha-tubulin. Mol. Biol. Cell 12, 2672–2687.

Chuang, H.Y., Chang, Y.F., Hwang, J.J., 2011. Antitumor effect of orlistat, a fatty acid synthase inhibitor, is via activation of caspase-3 on human colorectal carcinoma-bearing animal. Biomed. Pharmacother. 65, 286–292.

Coleman, D.T., Bigelow, R., Cardelli, J.A., 2009. Inhibition of fatty acid synthase by luteolin post-transcriptionally down-regulates c-Met expression independent of proteosomal/lysosomal degradation. Mol. Cancer Ther. 8, 214–224.

Daniels, V.W., Smans, K., Royaux, I., Chypre, M., Swinnen, J.V., Zaidi, N., 2014. Cancer cells differentially activate and thrive on de novo lipid synthesis pathways in a low-lipid environment. PLoS One 9, e106913.

Dean, E.J., Falchook, G.S., Patel, M.R., Brenner, A.J., Infante, J.R., Arkenau, H.T., Borazanci, E.H., Lopez, J.S., Pant, L.S., Schmid, P., Frankel, A.E., Jones, S.F., Mcculloch, W., Kemble, G., O'farrell, M., Burris, H., 2016. Preliminary activity in the first in human study of the first-in-class fatty acid synthase (FASN) inhibitor, TVB-2640. J. Clin. Oncol. 2512 (ASCO Meeting Abstracts).

Eisenberg, S., Laude, A.J., Beckett, A.J., Mageean, C.J., Aran, V., Hernandez-Valladares, M., Henis, Y.I., Prior, I.A., 2013. The role of palmitoylation in regulating Ras localization and function. Biochem. Soc. Trans. 41, 79–83.

Fiorentino, M., Zadra, G., Palescandolo, E., Fedele, G., Bailey, D., Fiore, C., Nguyen, P.L., Migita, T., Zamponi, R., Di Vizio, D., Priolo, C., Sharma, C., Xie, W., Hemler, M.E., Mucci, L., Giovannucci, E., Finn, S., Loda, M., 2008. Overexpression of fatty acid synthase is associated with palmitoylation of Wnt1 and cytoplasmic stabilization of beta-catenin in prostate cancer. Lab. Investig. 88, 1340–1348.

Flavin, R., Peluso, S., Nguyen, P.L., Loda, M., 2010. Fatty acid synthase as a potential therapeutic target in cancer. Future Oncol. 6, 551–562.

Gonzalez-Guerrico, A.M., Espinoza, I., Schroeder, B., Park, C.H., Kvp, C.M., Khurana, A., Corominas-Faja, B., Cuyas, E., Alarcon, T., Kleer, C., Menendez, J.A., Lupu, R., 2016. Suppression of endogenous lipogenesis induces reversion of the malignant phenotype and normalized differentiation in breast cancer. Oncotarget.

Hu, J., Che, L., Li, L., Pilo, M.G., Cigliano, A., Ribback, S., Li, X., Latte, G., Mela, M., Evert, M., Dombrowski, F., Zheng, G., Chen, X., Calvisi, D.F., 2016. Co-activation of AKT and c-Met triggers rapid hepatocellular carcinoma development via the mTORC1/FASN pathway in mice. Sci. Rep. 6, 20484.

Jensen-Urstad, A.P., Song, H., Lodhi, I.J., Funai, K., Yin, L., Coleman, T., Semenkovich, C.F., 2013. Nutrient-dependent phosphorylation channels lipid synthesis to regulate PPARalpha. J. Lipid Res. 54, 1848–1859.

Kridel, S.J., 2004. Orlistat is a novel inhibitor of fatty acid synthase with antitumor activity. Cancer Res. 64, 2070–2075.

Levental, I., Lingwood, D., Grzybek, M., Coskun, U., Simons, K., 2010. Palmitoylation regulates raft affinity for the majority of integral raft proteins. Proc. Natl. Acad. Sci. U. S. A. 107, 22050–22054.

Lingwood, D., Simons, K., 2010. Lipid rafts as a membrane-organizing principle. Science 327, 46–50.

Marien, E., Meister, M., Muley, T., Fieuws, S., Bordel, S., Derua, R., Spraggins, J., Van De Plas, R., Dehairs, J., Wouters, J., Bagadi, M., Dienemann, H., Thomas, M., Schnabel, P.A., Caprioli, R.M., Waelkens, E., Swinnen, J.V., 2015. Non-small cell lung cancer is characterized by dramatic changes in phospholipid profiles. Int. J. Cancer 137, 1539–1548.

Martin, B.R., Cravatt, B.F., 2009. Large-scale profiling of protein palmitoylation in mammalian cells. Nat. Methods 6, 135–138.

Menendez, J.A., Lupu, R., 2007. Fatty acid synthase and the lipogenic phenotype in cancer pathogenesis. Nat. Rev. Cancer 7, 763–777.

Menendez, J.A., Lupu, R., Colomer, R., 2004. Inhibition of tumor-associated fatty acid synthase hyperactivity induces synergistic chemosensitization of HER −2/ neu -overexpressing human breast cancer cells to docetaxel (taxotere). Breast Cancer Res. Treat. 84, 183–195.

Miura, G.I., Buglino, J., Alvarado, D., Lemmon, M.A., Resh, M.D., Treisman, J.E., 2006. Palmitoylation of the EGFR ligand Spitz by Rasp increases Spitz activity by restricting its diffusion. Dev. Cell 10, 167–176.

Nguyen, P.L., Ma, J., Chavarro, J.E., Freedman, M.L., Lis, R., Fedele, G., Fiore, C., Qiu, W., Fiorentino, M., Finn, S., Penney, K.L., Eisenstein, A., Schumacher, F.R., Mucci, L.A., Stampfer, M.J., Giovannucci, E., Loda, M., 2010. Fatty acid synthase polymorphisms, tumor expression, body mass index, prostate cancer risk, and survival. J. Clin. Oncol. 28, 3958–3964.

Notarnicola, M., Tutino, V., Calvani, M., Lorusso, D., Guerra, V., Caruso, M.G., 2012. Serum levels of fatty acid synthase in colorectal cancer patients are associated with tumor stage. J. Gastrointest. Cancer 43, 508–511.

Ozols, J., Caron, J.M., 1997. Posttranslational modification of tubulin by palmitoylation: II. Identification of sites of palmitoylation. Mol. Biol. Cell 8, 637–645.

Peck, B., Schug, Z.T., Zhang, Q., Dankworth, B., Jones, D.T., Smethurst, E., Patel, R., Mason, S., Jiang, M., Saunders, R., Howell, M., Mitter, R., Spencer-Dene, B., Stamp, G., Mcgarry, L., James, D., Shanks, E., Aboagye, E.O., Critchlow, S.E., Leung, H.Y., Harris, A.L., Wakelam, M.J., Gottlieb, E., Schulze, A., 2016. Inhibition of fatty acid desaturation is detrimental to cancer cell survival in metabolically compromised environments. Cancer Metab. 4, 6.

Puig, T., Vazquez-Martin, A., Relat, J., Petriz, J., Menendez, J.A., Porta, R., Casals, G., Marrero, P.F., Haro, D., Brunet, J., Colomer, R., 2008. Fatty acid metabolism in breast cancer cells: differential inhibitory effects of epigallocatechin gallate (EGCG) and C75. Breast Cancer Res. Treat. 109, 471–479.

Puig, T., Turrado, C., Benhamu, B., Aguilar, H., Relat, J., Ortega-Gutierrez, S., Casals, G., Marrero, P.F., Urruticoechea, A., Haro, D., Lopez-Rodriguez, M.L., Colomer, R., 2009. Novel inhibitors of fatty acid synthase with anticancer activity. Clin. Cancer Res. 15, 7608–7615.

Puig, T., Aguilar, H., Cufi, S., Oliveras, G., Turrado, C., Ortega-Gutierrez, S., Benhamu, B., Lopez-Rodriguez, M.L., Urruticoechea, A., Colomer, R., 2011. A novel inhibitor of fatty acid synthase shows activity against HER2+ breast cancer xenografts and is active in *anti*-HER2 drug-resistant cell lines. Breast Cancer Res. 13, R131.

Runkle, K.B., Kharbanda, A., Stypulkowski, E., Cao, X.J., Wang, W., Garcia, B.A., Witze, E.S., 2016. Inhibition of DHHC20-mediated EGFR palmitoylation creates a dependence on EGFR signaling. Mol. Cell 62, 385–396.

Rysman, E., Brusselmans, K., Scheys, K., Timmermans, L., Derua, R., Munck, S., Van Veldhoven, P.P., Waltregny, D., Daniels, V.W., Machiels, J., Vanderhoydonc, F., Smans, K., Waelkens, E., Verhoeven, G., Swinnen, J.V., 2010. De novo lipogenesis protects cancer cells from free radicals and chemotherapeutics by promoting membrane lipid saturation. Cancer Res. 70, 8117–8126.

Schug, Z.T., Peck, B., Jones, D.T., Zhang, Q., Grosskurth, S., Alam, I.S., Goodwin, L.M., Smethurst, E., Mason, S., Blyth, K., Mcgarry, L., James, D., Shanks, E., Kalna, G., Saunders, R.E., Jiang, M., Howell, M., Lassailly, F., Thin, M.Z., Spencer-Dene, B., Stamp, G., Van Den Broek, N.J., Mackay, G., Bulusu, V., Kamphorst, J.J., Tardito, S., Strachan, D., Harris, A.L., Aboagye, E.O., Critchlow, S.E., Wakelam, M.J., Schulze, A., Gottlieb, E., 2015. Acetyl-CoA synthetase 2 promotes acetate utilization and maintains cancer cell growth under metabolic stress. Cancer Cell 27, 57–71.

Sebastiani, V., Botti, C., Di Tondo, U., Visca, P., Pizzuti, L., Santeusanio, G., Alo, P.L., 2006. Tissue microarray analysis of FAS, Bcl-2, Bcl-x, ER, PgR, Hsp60, p53 and Her2-neu in breast carcinoma. Anticancer Res. 26, 2983–2987.

Shah, U.S., Dhir, R., Gollin, S.M., Chandran, U.R., Lewis, D., Acquafondata, M., Pflug, B.R., 2006. Fatty acid synthase gene overexpression and copy number gain in prostate adenocarcinoma. Hum. Pathol. 37, 401–409.

Simons, K., Sampaio, J.L., 2011. Membrane organization and lipid rafts. Cold Spring Harb. Perspect. Biol. 3, a004697.

Smans, K.A., De Breucker, S., Esser, N., Fraiponts, E., Gillissen, R., Graeser, R., Janssen, B., Meerpoel, L., Peeters, D., Van Hecke, G., Van Nuffel, L., Chong, Y., Vermeulen, P., Bignan, G., Bischoff, J., Connolly, P., Grasberger, B., Lu, T., Ludovivi, D., Schbert, C., Parker, M., Meyer, C., Vidic, S., 2014. Sensitivity of cell lines to fatty acid synthase inhibitors depends on the lipid content in the cellular environment. Cancer Res. 74 (Abstract nr 801).

Song, S.P., Hennig, A., Schubert, K., Markwart, R., Schmidt, P., Prior, I.A., Bohmer, F.D., Rubio, I., 2013. Ras palmitoylation is necessary for N-Ras activation and signal propagation in growth factor signalling. Biochem. J. 454, 323–332.

Tao, B.B., He, H., Shi, X.H., Wang, C.L., Li, W.Q., Li, B., Dong, Y., Hu, G.H., Hou, L.J., Luo, C., Chen, J.X., Chen, H.R., Yu, Y.H., Sun, Q.F., Lu, Y.C., 2013. Up-regulation of USP2a and FASN in gliomas correlates strongly with glioma grade. J. Clin. Neurosci. 20, 717–720.

Tomek, K., Wagner, R., Varga, F., Singer, C.F., Karlic, H., Grunt, T.W., 2011. Blockade of fatty acid synthase induces ubiquitination and degradation of phosphoinositide-3-kinase signaling proteins in ovarian cancer. Mol. Cancer Res. 9, 1767–1779.

Uddin, S., Hussain, A.R., Ahmed, M., Bu, R., Ahmed, S.O., Ajarim, D., Al-Dayel, F., Bavi, P., Al-Kuraya, K.S., 2010. Inhibition of fatty acid synthase suppresses c-Met receptor kinase and induces apoptosis in diffuse large B-cell lymphoma. Mol. Cancer Ther. 9, 1244–1255.

Ueda, S.M., Yap, K.L., Davidson, B., Tian, Y., Murthy, V., Wang, T.L., Visvanathan, K., Kuhajda, F.P., Bristow, R.E., Zhang, H., Iem, S.H.I.H., 2010. Expression of fatty acid synthase depends on NAC1 and is associated with recurrent ovarian serous carcinomas. J. Oncol. 2010, 285191.

Vander Heiden, M.G., Cantley, L.C., Thompson, C.B., 2009. Understanding the Warburg effect: the metabolic requirements of cell proliferation. Science 324, 1029–1033.

Vazquez-Martin, A., Colomer, R., Brunet, J., Lupu, R., Menendez, J.A., 2008. Overexpression of fatty acid synthase gene activates HER1/HER2 tyrosine kinase receptors in human breast epithelial cells. Cell Prolif. 41, 59–85.

Ventura, R., Mordec, K., Waszczuk, J., Wang, Z., Lai, J., Fridlib, M., Buckley, D., Kemble, G., Heuer, T.S., 2015. Inhibition of de novo palmitate synthesis by fatty acid synthase induces apoptosis in tumor cells by remodeling cell membranes, inhibiting signaling pathways, and reprogramming gene expression. EBioMedicine 2, 806–822.

Wan, J., Roth, A.F., Bailey, A.O., Davis, N.G., 2007. Palmitoylated proteins: purification and identification. Nat. Protoc. 2, 1573–1584.

Ward, P.S., Thompson, C.B., 2012. Metabolic reprogramming: a cancer hallmark even Warburg did not anticipate. Cancer Cell 21, 297–308.

Witkiewicz, A.K., Nguyen, K.H., Dasgupta, A., Kennedy, E.P., Yeo, C.J., Lisanti, M.P., Brody, J.R., 2008. Co-expression of fatty acid synthase and caveolin-1 in pancreatic ductal adenocarcinoma: implications for tumor progression and clinical outcome. Cell Cycle 7, 3021–3025.

Yeste-Velasco, M., Linder, M.E., Lu, Y.J., 2015. Protein S-palmitoylation and cancer. Biochim. Biophys. Acta 1856, 107–120.

Zambito, A.M., Wolff, J., 1997. Palmitoylation of tubulin. Biochem. Biophys. Res. Commun. 239, 650–654.

Zaytseva, Y.Y., Rychahou, P.G., Gulhati, P., Elliott, V.A., Mustain, W.C., O'connor, K., Morris, A.J., Sunkara, M., Weiss, H.L., Lee, E.Y., Evers, B.M., 2012. Inhibition of fatty acid synthase attenuates CD44-associated signaling and reduces metastasis in colorectal cancer. Cancer Res. 72, 1504–1517.